An experimental technique to evaluate the effective thermal conductivity of Y_2O_3 stabilized ZrO_2 coatings

K. AN*, M. K. HAN
Korea Institute of Industrial Technology, 994-32, Dongchun-Dong, Yeonsu-Gu, Incheon, Korea

An experimental device was set up to determine thermal resistance and conductivity of 8% yttria-stabilized zirconia deposited by plasma spray method on cylindrical specimen. In this experimental setup, coated surface of the sample was exposed to a high temperature environment and inner metal surface was cooled by flowing air, simulating actual gas turbine applications. Overall heat resistance at the outside surface of thermal barrier coating was adopted to assess thermal advantage due to the thermal barrier coating deposited on air-cooled cylindrical specimen. 28% less heat was extracted at 1000°C by applying 1.2 mm thick thermal barrier coating. Temperatures of the outside surface of the coated samples increased with increasing coating thickness with respect to the same furnace temperature since the sample with thicker coating was less thermally conductive and retarded heat transfer. The overall heat resistances of samples between the outside surface of sample and the flowing air inside the sample assembly were estimated. Then, the thermal conductivity of coating could be determined from the difference of overall thermal resistances of two selected samples with varying coating thickness.

1. Introduction

Thermal barrier coatings (TBCs) are applied to metallic components of a turbine blade to reduce the metal temperature and the high temperature corrosion, thereby increasing the operational life time of the component. TBCs are usually made of 8% yttria-stabilized zirconia (8YSZ) due to the low value of the thermal conductivity of 8YSZ relative to most other crystalline oxide ceramics. By applying 0.3–0.5 mm thick TBC to the hot side of the metal parts, the temperature of the metal can be reduced by at least a few hundred degrees [1]. Therefore, the underlying metal can operate at a higher temperature due to the temperature drop through the YSZ coating. This has an obvious advantage in the gas turbine engine, where the fuel efficiency is proportional to the maximum temperature in the combustion chamber that can be tolerated. The thicker the ceramic coating, the higher the operating temperature that can be allowed in the combustion zone and hence the more efficient use of fuel in the engine. In general, the thermal resistance, or specifically, the thermal conductivity of the TBC is an important parameter that is often considered in the design.

Frequently, thermal conductivity of materials is determined by the laser flash method [2]. This involves the determination of thermal diffusivity, specific heat and density independently. Thermal conductivity is then given as a function of thermal diffusivity, specific heat and density. There can be a number of issues concerning the measurement of thermal diffusivity (and the thermal conductivity determination) and its use in designing TBCs. One of the problems is that thermal diffusivity measurements may be inaccurate due to the transparency of coatings at high temperatures. This is indicated by a study which showed that thermal conductivity of ZrO_2 coatings is sensitive to the specimen thickness [3]. To minimize this problem, thermal diffusivity of TBCs is usually determined after depositing a carbon black coating to reduce the effect of transparency of the coatings. Secondly, in actual gas turbine applications, the coating is partially transparent at the operating temperatures which is usually in the range of 900–1000°C. In addition to heat transfer by conduction (phonon transport), radiation (photon transport) would be expected to contribute significantly to the overall heat transfer [4]. Therefore, thermal conductivity alone does not completely represent the heat transfer mechanism in TBCs but all modes of heat transfer including conduction, convection and radiation contributes to the thermal conductivity. Since radiation

*Author to whom all correspondence should be addressed.
0022-2461
DOI: 10.1007/s10853-006-3144-3

is invariably a part of the overall heat transfer in gas turbines, it may be more appropriate to measure the thermal conductivity of selected TBCs under conditions that are similar to the gas turbine engines. In addition, in the conventional laser flash thermal diffusivity measurements on coatings with the substrates, there is a degree of uncertainty arising from the thermal resistance due to imperfect interface between the coating and the substrate. This contact thermal resistance also depends on the pressure with which contact is maintained, the thermal and physical properties of the mating materials, and actual contact area which is a function of interface surface roughness [5–7].

The approach is based on an experimental set-up in which one surface of the coating is exposed to a high temperature environment and heat is extracted from the other side by flowing air. This arrangement could be set-up in a laboratory. By measuring the overall thermal resistances of coatings of various thicknesses, it has been shown that the thermal conductivity of a segment of the coating can be determined by the differences in thermal resistances of two specimens with varying coating thickness.

One of objectives of the present work is to extract the thermal conductivity of the thermal barrier coatings under conditions that are nearly the same as the actual application. It is also of interest to see if the thermal conductivity of coating can be affected by applying different coating thicknesses, as well as, if the thermal conductivity of coating estimated from the differences of thermal resistances will be the same as that of measured by laser flash method.

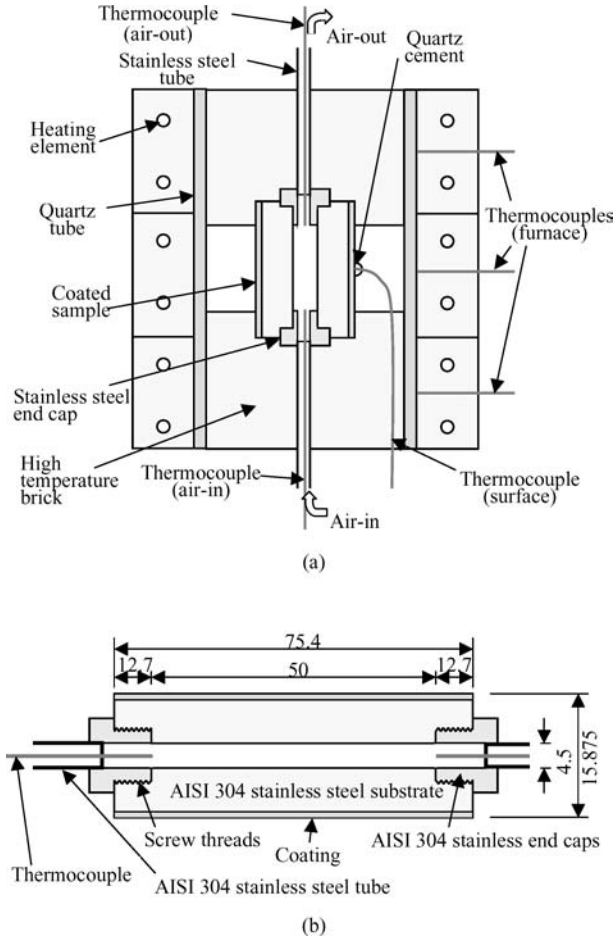

Figure 1 Schematics of (a) the overall experimental setup and (b) the cylindrical sample assembly for thermal resistance and conductivity measurement.

2. Experimental procedures

Fig. 1a shows the experimental setup device. The threaded ends of the samples were protected by insulating bricks in order to minimize heat loss in the axial direction of the sample. A three-zone resistance heating furnace (model no. 54357, Lindberg) was used in the experiment. The heating chamber of furnace accommodated a quartz tube of 70 mm outer diameter and 55 mm inner diameter. The sample assembly in Fig. 1b and bricks were placed in this quartz tube. The bricks on both sides served to support the sample assembly as well as to protect the tube, caps and sample threads from exposure to high temperature. Stainless steel tubes of 4.57 mm inner and 6.35 mm outer diameter were used to carry cooling air.

Two thermal couples were placed inside sample passing through the stainless steel tubes. Their tip-to-tip distance was 50 mm in order to measure the inlet and the outlet temperatures of flowing air through the sample. Care was taken to ensure that these thermocouples did not touch the tube wall. The temperature of sample surface was measured by another thermocouple located on the specimen midlength. For this purpose, a thermocouple was bonded at this location using quartz cement (Thermal American Fused Quartz Co.) made by mixing 25% filler (powder) and 75% binder (liquid). Then, the thermocouple-sample bond was allowed to dry for 24 hrs. The quarts bond provided a sound contact between thermocouple and sample surface. The furnace temperature was also monitored by a thermocouple. The measurements were made at every 100°C increment from 200 to 1000°C on the basis of furnace temperature and duration time at each temperature step was 3 hrs to ensure steady-state heat transfer condition.

Sample assembly of 75.4 mm in length, 4.57 mm in inner diameter and 15.875 mm in outer diameter was made of AISI 304 stainless steel cylindrical substrate and TBC on it (Fig. 1b). In addition, the sample consisted of 12.7 mm screw threads at both of its ends and 50 mm-middle part for thermal analysis. A steady-state heat transfer was assured by the concentric cylinder design and temperature is a function of only the radial coordinate r.

Four samples with different coating thickness from 0.4 to 2 mm were prepared for the present study (Table I). Prior to the deposition of these coatings, the outer diameter of the 304 stainless steel cylindrical substrate was selected such that the total diameter was 15.875 mm in all the samples. For instance, to make the sample with 1.2 mm thick coating, the outer diameter of cylindrical substrate was selected as 13.475 mm and then plasma spraying was performed to deposit a

TABLE I Descriptions, substrate diameter and coating thickness of cylindrical samples

Coating type	Substrate diameter (mm)	Coating thickness (mm)	Total diameter (mm)
0.4 mm coating + substrate	15.075	0.4	15.875
0.8 mm coating + substrate	14.275	0.8	15.875
1.2 mm coating + substrate	13.475	1.2	15.875
2.0 mm coating + substrate	11.875	2.0	15.875

coating of 1.2 mm in thickness using powders of 8% yttria-stabilized zirconia (8YSZ, Metco 204NS; average particle size: 2 μm). A Plasma Technik Spray system with a single spray nozzle and dual powder feeder available at the Thermal Spray Laboratory of the State University of New York, Stony Brook, NY was used. Calibration sprays were performed to control the layer thickness during the actual spray deposition. AISI 304 stainless steel tube does not pass through sample (Fig. 1b) but tightly fitted to the sample via AISI 304 stainless steel end caps. The screw threads between the sample and the end caps were designed to seal air completely. The sample-tube arrangement was rigid even at high temperature, since the thermal expansion coefficient of sample, caps and tube were identical. In gas turbines, the turbine blades are internally cooled by circulating air through the pathways inside the blade. This mode of heat extraction is closely simulated by the present study except for the air flow rate and convection heat transfer coefficient.

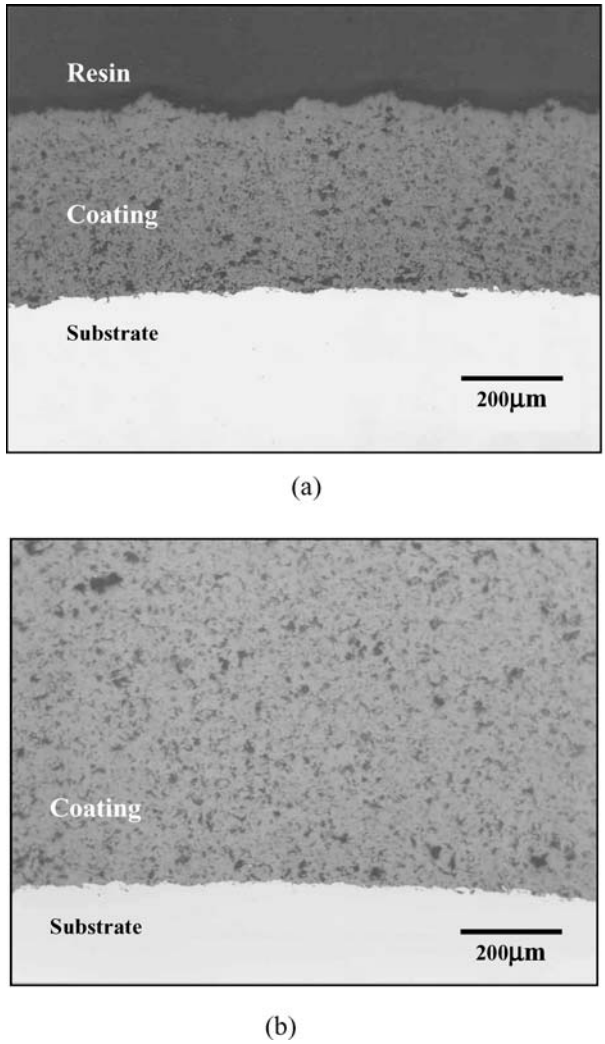

Figure 2 The microstructure of coatings of (a) 0.4 mm and (b) 1.2 mm in thicknesses after experiment.

3. Results and discussions

3.1. Microstructure of coatings

Fig. 2a and b show the microstructures of coatings of selected samples (0.4 and 1.2 mm coating samples) after the experiments. The microstructure of 12% porosity was similar to that observed before the coating was exposed to high temperature, suggesting that there was no change in the microstructure during the experiment. In all of the coated samples, the coatings were well bonded to underlying metal without any visible crack before and after the thermal measurements. There is no doubt that the contact between the coating and the substrate was maintained rigid during experiments. The fit at the interface between the coating and the substrate might be improved at high temperature since the expansion coefficient of 304 stainless steel substrate is greater than that of 8YSZ coating.

3.2. Characterization of air flowing through sample

The amount of extracted heat by flowing air through sample strongly depends on velocity of air flowing and tube diameter in the tube. The Reynolds number is used to characterize flowing air inside sample. Therefore, since thermal resistance and thermal conductivity were calculated from the amount of heat extraction by flowing air through sample, the Reynolds number should be analyzed in advance involving the determination of thermal resistance and thermal conductivity. Heat transfer rate tends to be much higher in turbulent flow than in laminar flow, owing to the vigorous mixing of the air in the tube [7, 8]. In this condition, the temperature of flowing air in the sample strongly depends on the temperature of inner surface of metal substrate. The degree of turbulence can be assessed using Reynolds number. The Reynolds numbers is determined by

$$\mathrm{Re} = VD/\nu \quad (1)$$

where V is the velocity of the flowing air (m/s), D is inner diameter of the sample (m), and ν is kinematic viscosity of air (m^2/s). The volumetric flow rate of air-in was maintained 2.4 m^3/hr at room temperature. The air temperature inside the sample (T_{air}), averaging T_{in} and T_{out} was used

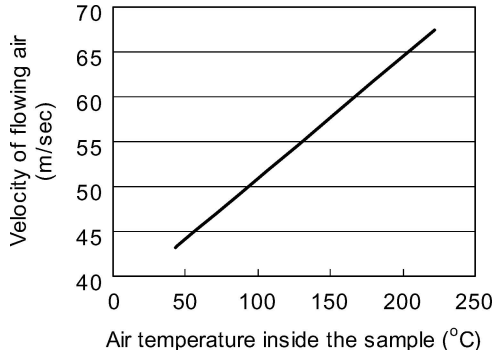

Figure 3 The velocity of flowing air through the sample is a function of the air temperature inside sample.

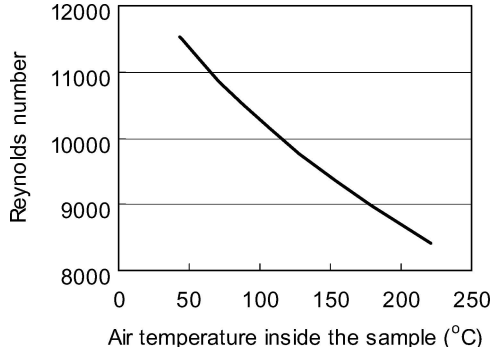

Figure 4 Reynolds number as a function of air temperature flowing through sample.

to calculate the velocity of flowing air through the sample. The velocity of flowing air through the sample is a function of T_{air} as shown in Fig. 3. The calculated Reynolds numbers indicated that the air flowing was in nearly fully-turbulent condition as shown in Fig. 4 since air flow in a pipe became turbulent when the Reynolds number exceeds about 2300. T_{air} of all the samples varied in the range of 40 to 210°C in entire range of heating cycle from 200 to 1000°C. The efficient convective heat transfer by turbulent flow was established to cool down the sample. The data of the thermophysical properties for Reynolds number are taken from literature [7].

3.3. Temperature of flowing air

Fig. 5 shows the temperatures of air-in (T_{in}) and out (T_{out}) through the samples with different coating thicknesses. T_{out} decreased as coating thickness increased at a given furnace temperature while T_{in} was not affected largely and thereby, the average air temperature (T_{air}) decreased as the thickness of coating increased. With increase in coating thickness, the decrease of the difference (ΔT_{air}) between T_{in} and T_{out} suggested that less heat was extracted. The temperatures of outside surface of samples (T_{surf}) increased with coating thickness at a given furnace temperature (Fig. 6). The sample with thicker coating was more heat resistive and retarded heat transfer. The accumulated heat at the outside surface of thicker coating affected the

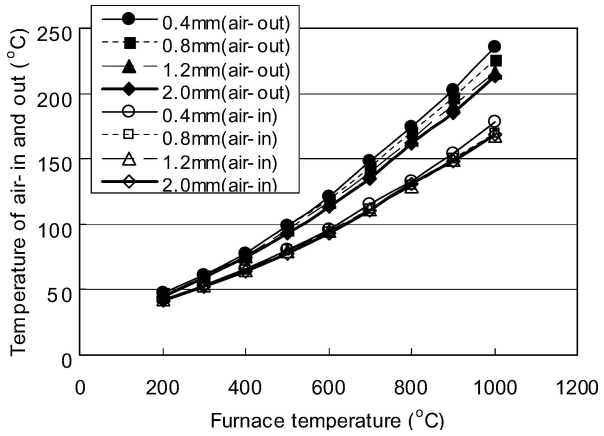

Figure 5 Temperatures of air-in and out with furnace temperature.

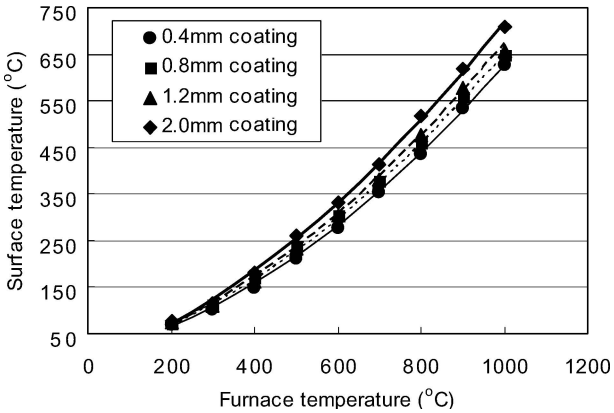

Figure 6 Temperatures of coated sample surface with furnace temperature.

surface temperature, resulting in that the surface temperature increased with coating thickness. Thermal resistance as well as thermal conductivity of the coatings can be calculated from the idea that T_{out}, T_{in} and T_{surf} at a given furnace temperature varies only as a function of coating thickness.

3.4. Determination of thermal resistance

The heat flux, Q, in the radial direction of the sample is identical with the amount of heat extraction in the axial direction by flowing air through the sample. This is given by

$$Q = \dot{m}\, C_p\, \Delta T_{air}\,(\mathrm{W}) \tag{2}$$

where $\dot{m}$ is the mass flow rate (kg/sec) that is a product of the volumetric flow rate (m^3/sec) and the density of air (kg/m^3). Cp is the specific heat of air (J/kg·K), and ΔT_{air} is the temperature difference (K) between air-in and out through the sample. The amount of heat extraction by flowing air directly proportional to the temperature differences between air-in and out under constant the mass flow rate of 7.85×10^{-4} kg/sec (the volumetric flow rate at room temperature; 2.4 m^3/hr). The results of heat flux

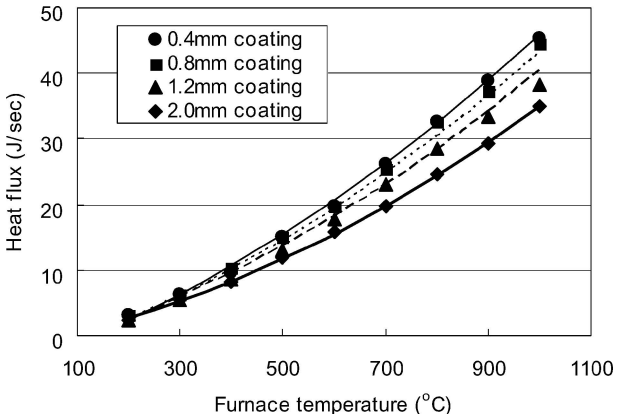

Figure 7 Heat flow rate with furnace temperature.

are shown in Fig. 7. The heat flux in each sample increased with furnace temperature but decreased with the coating thickness. The heat fluxes through 0.8, 1.2 and 2.0 mm coating samples at 1000°C of furnace temperature were 98, 84 and 77% of that of 0.4 mm coating sample.

Thermal barrier coating affected the amount of heat extraction as well as the temperature gradient between inside and outside surface of sample at the same horizontal level. In the view of the point, the overall thermal resistance between the outside surface of sample and the flowing air inside sample can be more effective to characterize the contribution of thermal barrier coating. To assess the overall thermal advantage through thermal barrier coating with varying thickness, the sample assembly consisting of 8YSZ, metal substrate and flowing air inside sample was treated as a unit of composite cylindrical shell with convection, conduction and radiation. The complexity of the radiation and convection through the air layer outside sample precludes exact thermal analysis and differs far from the conduction condition [6, 7]. To ignore the uncertainty of radiation, all of the samples were under the equivalent geometrical condition having 8YSZ coating layer with the same outer diameter of 15.875 mm so that they had the same emissivity of radiation. Then, the overall thermal resistance of a sample was subtracted by the other to eliminate the radiation effect. Also, the overall thermal resistance from the outer surface mounted by thermocouple to inner flowing air was used for the thermal evaluation in order to neglect the convection effect of the air layer at the outer surface. Therefore, thermal analysis of radiation and convection at the outer sample surface was not taken into account for the present study.

The overall thermal resistance (or the summation of all the resistances in the series network) can be estimated from the amount of heat extraction and the temperature gradient. The overall thermal resistance was expressed by following equations [7, 8]

$$R = \frac{T_{\text{surf}} - T_{\text{air}}}{Q} \text{ (K/W)} \qquad (3)$$

and

$$R = \frac{1}{2\pi L} \sum \left(\frac{1}{r_i h_i} + \frac{\ln(r_o/r_i)}{k_i} \right) \text{(K/W)} \qquad (4)$$

where R is the overall thermal resistance and T_{surf} is the surface temperature of coatings and T_{air} is the average air temperature of flowing air inside sample. r_i and r_o are the inside and the outside radius of sample, respectively. k_i is the thermal conductivity of a sample. For a cylindrical shell of length L and inner radius r, the area for heat flow is $2\pi rL$. For instance, thermal resistance of 2.0 mm coating sample at 1000°C of furnace temperature can be calculated flowing procedure,

$$Q_{2.0} = 7.85 \times 10^{-4}\,\text{kg/sec} \times 1014.12\,\text{J/kg K} \times (213 - 169)\,\text{K} = 35.03\,\text{W}$$

and

$$R_{2.0} = \frac{(710 - 191)\,\text{K}}{35.03\ \text{W}} = 14.82\,\text{K/W}$$

In Fig. 8, the overall thermal resistance of each coated sample increased with the furnace temperature. Multiple regression analysis using data points of thermal resistance, furnace temperature and coating thickness was done. From the results of the multiple regression analysis, the thermal resistance increased linearly with the furnace temperature and the coating thickness except two data points at 200°C of 1.2 mm coating thickness and 300°C of 2.0 mm coating thickness. They were found to be outliers from this analysis and marked as open symbols. In addition, the sample with thicker coating had higher thermal resistance, suggesting that the thermal barrier coatings contributed to increase thermal resistance. The thermal resistances of 0.8, 1.2 and 2.0 mm coating samples at 1000°C of furnace temperature were higher than that of 0.4 mm coating sam-

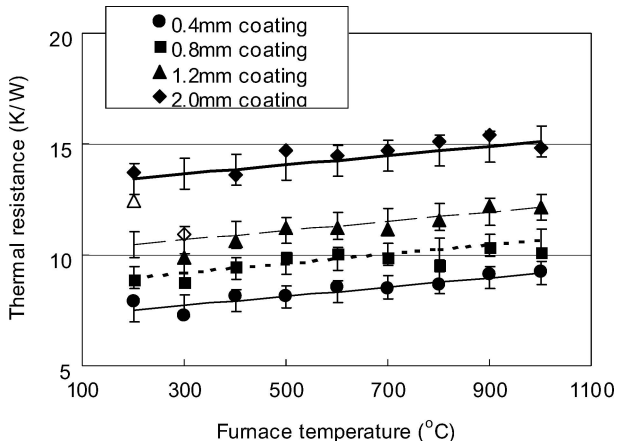

Figure 8 Thermal resistance at the coating surface to the air inside the sample.

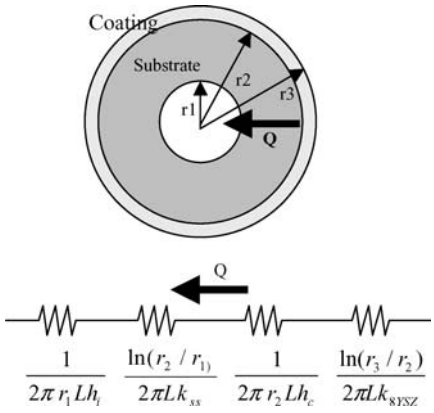

Figure 9 A schematic of cross section of cylindrical sample and thermal circuit in a radial direction of sample.

ple by factors of 1.1, 1.3 and 1.6. There are a few benefits by adapting the concept of the overall thermal resistance. Firstly, the uncertainty of the thermal contact resistance between coating and substrate can be ignored. In a realistic situation, there is always a contact resistance between two different materials [5–7]. Typical thermal conductance of interfaces between ceramics and metals is known to be in the range of 1500–8500 W/m^2 K depending on contact pressure [7]. Secondly, the convective heat transfer coefficient of flowing air inside the sample which is also complicated and unreliable does not need to be determined. Therefore, all we need is the overall heat resistance for thermal-conductivity calculation without specifying individual resistance.

3.5. Analysis and determination of thermal conductivity

Fig. 9 shows the schematics of the cross section of the sample and the thermal circuit. The sample considering as two layers composite includes stainless-steel substrate with r_1, r_2 and k_{ss}, and 8YSZ coating with r_2, r_3 and k_{8YSZ}, of inner radius, outer radius, and thermal conductivity, respectively. R is overall thermal resistance including the convection term of flowing air inside sample, the conduction term of stainless steel substrate, interface contact resistance term, and the conduction term of 8YSZ coating given by (see Equation 4)

$$R = \frac{1}{2\pi L}\left[\frac{1}{r_1 h_i} + \frac{\ln\left(\frac{r_2}{r_1}\right)}{k_{ss}} + \frac{1}{r_2 h_c} + \frac{\ln\left(\frac{r_3}{r_2}\right)}{k_{8YSZ}}\right] (\mathrm{K/W}) \tag{5}$$

where h_i and h_c are convection heat transfer coefficient of flowing air inside sample and contact resistance between the substrate and the coating, respectively. k_{ss} and k_{8YSZ} are the thermal conductivities of stainless-steel substrate and 8YSZ coating, respectively.

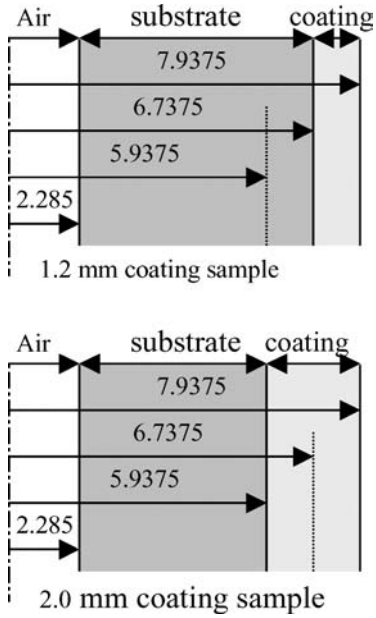

Figure 10 The comparison of the layer structure and its radius between 1.2 and 2.0 mm coating samples.

Thermal conductivities of coatings can be estimated from the differences of two overall thermal resistances. The assumption is that individual resistance terms are not effected by varying coating thickness since the microstructure of the samples were not changed with coating thickness. For instance, the comparison of the layer structure and its radius between 1.2 and 2.0 mm coating samples are shown in Fig. 10. Dot line is nothing but imaginary line to distinguish the 'transition volume' from stainless steel to 8YSZ. The volume of radius from 5.9375 to 6.7375 mm belongs to stainless steel substrate of 1.2 mm coating sample but is a part of 8YSZ coating of 2.0 mm coating sample. Therefore, the difference of the overall thermal resistances between 1.2 and 2.0 mm coating samples can be assumed to come from the thermal resistance difference of this 'transition volume'. From Fig. 10, the thermal resistances of 1.2 and 2.0 mm coating samples can be considered as the sum of series resistances given by (see Equation 5)

$$R_{1.2} = \frac{1}{2\pi L}\left(\frac{1}{2.285 h_i} + \frac{\ln\left(\frac{5.9375}{2.285}\right)}{k_{ss}} + \frac{\ln\left(\frac{6.7375}{5.9375}\right)}{k_{ss}} + \frac{1}{6.7375 h_c} + \frac{\ln\left(\frac{7.9375}{6.7375}\right)}{k_{8YSZ}}\right) \tag{6}$$

and

$$R_{2.0} = \frac{1}{2\pi L}\left(\frac{1}{2.285 h_i} + \frac{\ln\left(\frac{5.9375}{2.285}\right)}{k_{ss}} + \frac{1}{5.9375 h_c} + \frac{\ln\left(\frac{6.7375}{5.9375}\right)}{k_{8YSZ}} + \frac{\ln\left(\frac{7.9375}{6.7375}\right)}{k_{8YSZ}}\right) \tag{7}$$

where L is the length of sample for thermal analysis (0.05 m). Subtracting Equation 6 from Equation 7:

$$R_{2.0} - R_{1.2} = R_{1220} = \frac{\ln\left(\frac{6.7375}{5.9375}\right)}{2\pi L}\left(\frac{1}{k_{8YSZ}} - \frac{1}{k_{ss}}\right) \text{(K/W)} \quad (8)$$

where k_{ss} is the thermal conductivity of stainless steel. Contact resistance terms of 1×10^{-2} K/W scale after subtracting each other was so minimal by a factor of 0.01 relative to conductivity terms that it was neglected. R_{1220} is the difference of two overall thermal resistances of 1.2 and 2.0 mm coating samples. It can be also counted as the difference of the thermal resistances between stainless steel and 8YSZ in the volume of radius from 5.9375 to 6.7375 mm. Six of the thermal-resistance differences such as R_{0408}, R_{0412}, R_{0420}, R_{0812}, R_{0820}, and R_{1220} can be produced in the same manner out of four different overall thermal resistances ($R_{0.4}$, $R_{0.8}$, $R_{1.2}$ and $R_{2.0}$).

The thermal conductivity of 8YSZ coating, k_{8YSZ}, can be estimated from the difference of the overall thermal resistances (see equation 8). k_{8YSZ} determined from the difference of overall thermal-resistances, $R_{1.2}$ and $R_{2.0}$, can be especially denoted as k_{1220}, given by

$$k_{1220} = \left[\frac{2\pi L(R_{2.0} - R_{1.2})}{\ln\left(\frac{6.7375}{5.9375}\right)} + \frac{1}{k_{ss}}\right]^{-1} \text{(W/K)} \quad (9)$$

At 1000°C of furnace surface temperature (T_{surf}), $R_{1.2}$ and $R_{2.0}$ were 12.15 and 14.82 K/W, respectively, in Fig. 8 and k_{ss} was 27.6 W/mK taken from the literature [7]. k_{1220} at 1000°C was determined as 0.15 W/mK. In the same manner, thermal conductivities of 8YSZ at a given coating temperature can be calculated from six different combinations out of 0.4, 0.8, 1.2, and 2.0 mm coating samples (Fig. 11). These thermal conductivities estimated from the differences of thermal resistances were much smaller than those of as-sprayed free standing ZrO_2 measured by laser flash method by a factor of 0.1 even though they have the same microstructure made by plasma spray deposition.

Thermal conductivities of coatings of the present experiments varied 0.1 to 0.2 W/mK while those by laser flash method in literature [9, 10] varied from 1 to 1.4 W/mK. By taking 1–1.4 W/mK as thermal conductivity of coating layer, the thermal resistance of coating contributed only 5% to overall thermal resistance of Fig. 8. From this calculation, the contribution of coating is so negligible that there is no need to apply it as thermal barrier purpose. However, in the present experiment simulating the reality, thermal resistance of coating contributed approximately 28% to overall thermal resistance of 1.2 mm coating sample. For instance, individual thermal resistance of 1.2 mm

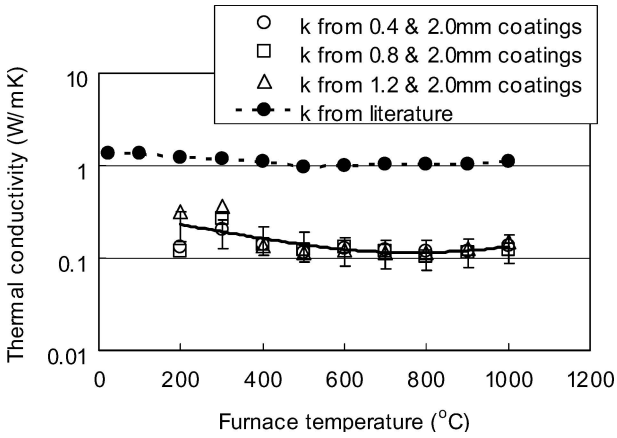

Figure 11 Thermal conductivities of coatings and their comparison to that in literature.

coating layer is given by

$$R_{8YSZ} = \frac{1}{2\pi L}\frac{\ln\left(\frac{7.9375}{6.7375}\right)}{k_{8YSZ}} = \Delta T/Q \quad (10)$$

By taking 0.15 W/mK as thermal conductivity determined by the present study, R_{8YSZ} was 3.48 K/W and its contribution was more than 28% to overall thermal resistance of 12.15 K/W at 1000°C of furnace temperature, giving 133°C temperature drop through coating layer of 1.2 mm. This analysis simulating the reality can be reasonable because a significant increment of thermal resistance was found when the thickness of thermal barrier coating increased, which is consistent with results in the literature (1, 7). However, the other individual resistances of the residual 72% were not clear for the present study. Those could be from flowing air inside sample, air layer on the coating surface and contact interface between coating and substrate.

4. Conclusions

(1) An experimental device was set-up to determine thermal resistance and conductivity of 8% yttria-stabilized zirconia deposited by plasma spray method on air-cooled cylindrical specimen. In this experimental setup, one surface of the coating is exposed to a high temperature environment and heat is extracted from the other side by flowing air, simulating actual gas turbine applications

(2) Less heat was extracted through thicker thermal barrier coating without increasing the temperature of metal blade, suggesting that thicker coating is more effective to increase the firing temperature without increasing underlying metal temperature, which allows the greater engine efficiency.

(3) The overall thermal resistance between the outside surface of sample and the flowing air inside sample was estimated from the amount of heat extraction and the temperature gradient in radial direction of sample. The overall heat resistance increased with coating thickness,

suggesting that the thermal barrier coatings contributed to increase thermal resistance.

(4) The effective thermal conductivity of 8YSZ coating, k_{8YSZ}, could be estimated from the difference of the overall thermal resistances. These effective thermal conductivities estimated from the differences of thermal resistances were 0.1 to 0.2 W/mK, that were much smaller than 1–1.4 W/mK of as-sprayed free standing ZrO_2 measured by laser flash method and even smaller than 2.3 W/mK of dense YSZ from literature (9).

References

1. M. P. BOROM and C. A. JOHNSON, *Surf. Coat. Technol.* **54/55** (1992) 45.
2. R. E. TAYLOR, *J. Phy. E. Sci. Inst.* **13** (1980) 1193.
3. A. RUDAJEVOVA, *Thin Solid Films* **223** (1993) 248.
4. M. A. STUBBLEFIELD, S. S. PANG and V. A. CUNDY, *Compos. Part B* **27B** (1996) 85.
5. E. FRIED, "Thermal Conduction Contribution to Heat Transfer at Contacts," vol. 2, edited by R. P. Tye (Academic Press, London and New York, 1969) p. 253.
6. A. F. MILLS, "Heat Transfer," International student ed. (D. RICHARD Irwin Inc., Concord, MA, 1992) p. 13.
7. G. D. SMITH, *J. Engng. Gas Turb. Power* **113** (1991) 35.
8. M. JAKOB and G. A. HAWKINS, "Elements of Heat Transfer" 3rd edn. (Wiley, New York, 1957) p. 33.
9. W. D. KINGERY, "Property Measurements at High Temperatures" (Wiley, New York, 1959).
10. K. S. RAVICHANDRAN and K. AN, *J. Amer. Ceram. Soc.* **82**(3) (1999) 673.

Received 30 October 2003
and accepted 9 May 2005